

Aging in a Chaotic System

Eli Barkai

Department of Chemistry,
Massachusetts Institute of Technology,
Cambridge, MA 02139.

(November 16, 2018)

Abstract

We demonstrate aging behavior in a simple non-linear system. Our model is a chaotic map which generates deterministically sub-diffusion. Asymptotic behaviors of the diffusion process are described using aging continuous time random walks, introduced previously to model diffusion in glasses.

Pacs numbers: 05.45.-a, 02.50-r, 05.60-k

Aging behavior is found in complex dynamical systems like spin glasses, glasses, and polymers [1]. These systems include many interacting sub-units and are disordered. In this letter we will demonstrate that aging can be found also in low dimensional non-linear systems. Specifically we will show that deterministic diffusion generated by one dimensional maps exhibits aging. And that statistical properties of the corresponding trajectories can be analyzed using aging continuous time random walks (ACTRW), introduced by Monthus and Bouchaud [2] in the context of aging dynamics in glasses (see also [3] and Ref. therein).

There exist several methods to investigate aging. One method is to start a dynamical process at time $t = -t_a$, then at time $t = 0$ add a small perturbation to the system. One eventually measures the response at some time $t > 0$. Alternatively one can measure correlation functions between physical quantities at time $t = 0$ and time t , after aging the system in the interval $(-t_a, 0)$. We use the latter approach. A system exhibits aging if its dynamical properties depend on t and t_a even in the limit when both are long. Of-course many systems do not exhibit aging, namely when $t > \tau$, where τ is a characteristic time scale of the problem, dynamical properties of the system are independent of the aging time t_a .

In many cases trajectories generated by deterministic systems, such as low dimensional Hamiltonians or maps, are highly irregular and noisy. For an observer these trajectories seem to be generated by a stochastic; rather than a deterministic mechanism. Hence analysis of chaotic trajectories generated deterministically is often based on random walk concepts [4–6]. It is well known [7] that both conservative and dissipative deterministic systems may generate normal ($\alpha = 1$) or anomalous ($\alpha \neq 1$) diffusion for a coordinate x

$$\langle x^2 \rangle \sim t^\alpha, \quad (1)$$

where the average is over a set of initial conditions (see

details below). The anomalous behavior is due for example to long trapping events in vicinity of unstable fixed points [8,9] or stickiness near islands in phase space [10]. Here we shall investigate a deterministic system which generates sub diffusion behavior $\alpha < 1$ and show how rich dynamical features emerge when aging is included. More generally, we demonstrate that aging can be used to probe dynamics in deterministic systems.

Probably the simplest theoretical tool which generates normal and anomalous diffusion are one dimensional maps

$$x_{t+1} = x_t + F(x_t) \quad (2)$$

with the following symmetry properties of $F(x)$: (i) $F(x)$ is periodic with a periodicity interval set to 1, $F(x) = F(x + N)$, where N is an integer. (ii) $F(x)$ has inversion anti-symmetry; namely, $F(x) = -F(-x)$. The study of these maps was motivated by the assumption that they capture essential features of a driven damped motion in a periodic potential [11]. Geisel and Thomae [8] considered a rather wide family of such maps which behave as

$$F(x) = ax^z \quad \text{for } x \rightarrow +0, \quad (3)$$

where $z > 1$. Variations of these maps have been investigated by taking into account: time dependent noise [12], quenched disorder [13], and additional uniform bias which breaks the symmetry of the map [14]. We use the map

$$F(x) = (2x)^z, \quad 0 \leq x \leq \frac{1}{2} \quad (4)$$

which together with the symmetry properties of the map define the mapping for all x . In Fig. 1 we show the map for three unit cells.

To investigate aging, e.g. numerically, we choose an initial condition x_{-t_a} which is chosen randomly and uniformly in the interval $-1/2 < x_{-t_a} < 1/2$. The quantity of interest is the displacement in the interval $(0, t)$, $x = x_t - x_0$ which is obtained using the map Eq. (2). Previous work [8,15] considered the non-aging regime, namely $t_a = 0$.

In an ongoing process a walker following the iteration rules may get stuck close to the vicinity of unstable fixed points of the map (see Fig. 1). It has been shown, both analytically and numerically, that probability density function (PDF) of escape times of trajectories from the vicinity of the fixed points decays like a

power law [8]. To see this one considers the dynamics in half a unit cell, say $0 < x < 1/2$. Assume that at time $t = 0$ the particle is on x^* residing in vicinity of the the fixed point $x = 0$. Close to the fixed point we may approximate the map Eq. (2) with the differential equation $dx/dt = F(x)$. Hence the escape time from x^* to a boundary on b ($x^* < b < 1/2$) is

$$t \simeq \int_{x^*}^b \frac{dx}{F(x)} \quad (5)$$

using Eq. (3)

$$t \simeq \frac{1}{a} \left[\frac{x^{*-z+1}}{z-1} - \frac{b^{-z+1}}{z-1} \right]. \quad (6)$$

The PDF of escape times $\psi(t)$ is related to the unknown PDF of injection points $\eta(x^*)$, through the chain rule $\psi(t) = \eta(x^*)|dx^*/dt|$. Expanding $\eta(x^*)$ around the unstable fixed point $x^* = 0$ one finds that for large escape times

$$\psi(t) \sim \frac{A}{\Gamma(-\alpha)} t^{-1-\alpha}, \quad \alpha = \frac{1}{(z-1)}, \quad (7)$$

where A depends on the PDF of injection points. Note that when $z > 2$ corresponding to $\alpha < 1$, the average escape time diverges.

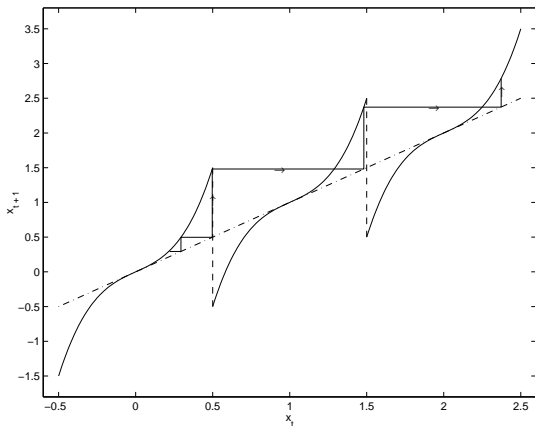


FIG. 1. The map $x_{t+1} = x_t + F(x_t)$, defined by Eq. (4) with $z = 3$. The linear dash-dot curve is $x_{t+1} = x_t$. The unstable fixed points are on $x_t = 0, 1, 2$.

To consider stochastic properties of the aging dynamics we investigate now ACTRW, deriving an explicit expression for the asymptotic behavior of the Green function. Specifically we consider a one-dimensional nearest neighbor random walk. Each lattice point corresponds to a cell of the iterated maps. Waiting times on each lattice point are assumed to be described by $\psi(t)$. Note that after each jumping event we assume that the process is renewed, namely, we neglect correlation between motions in neighboring cells. This assumption will be justified

later using numerical simulations. As mentioned start of the ACTRW process is at $t = -t_a$ and our goal is to find the ACTRW Green function $P(x, t_a, t)$.

In ACTRW we must introduce the distribution of the first waiting time t_1 : the time elapsing between start of observation at $t = 0$ and the first jump event in the interval $(0, t)$. Let $h_{t_a}(t_1)$ be the PDF of t_1 . Let $h_s(u)$ be the double Laplace transform of $h_{t_a}(t_1)$

$$h_s(u) = \int_0^\infty dt_1 \int_0^\infty dt_a h_{t_a}(t_1) e^{-t_a s - t_1 u}, \quad (8)$$

then according to theory of fractal renewal processes [16]

$$h_s(u) = \frac{1}{1 - \psi(s)} \frac{\psi(s) - \psi(u)}{u - s}. \quad (9)$$

When $\alpha < 1$ in Eq. (7) (i.e., $z > 2$)

$$h_{t_a}(t_1) \sim \frac{\sin(\pi\alpha)}{\pi} \frac{t_a^\alpha}{t_1^\alpha (t_1 + t_a)}, \quad (10)$$

which is valid in the long aging time limit $t_a \gg A^{1/\alpha}$. Note that Eq. (10) is independent of the exact form of $\psi(t)$, besides the exponent α . When $\alpha \rightarrow 1$ the mass of the PDF $h_{t_a}(t_1)$ is concentrated in the vicinity of $t_1 \rightarrow 0$, as expected from a ‘normal process’. In what follows we will also use the double Laplace transform of Eq. (10)

$$h_s(u) \sim \frac{u^\alpha - s^\alpha}{s^\alpha(u - s)}. \quad (11)$$

We have checked numerically the predictions of Eq. (10) for $z = 3$, analyzing trajectories generated by the map Eq. (4) with three different aging times. In Fig. 2 we show the probability of making at-least one step in the interval $(0, t)$: $\int_0^t h_{t_a}(t) dt \equiv 1 - p_0(t_a, t)$. The results show a good agreement between numerical results and the theoretical prediction Eq. (10) without fitting. Fig. 2 clearly demonstrates that as the aging time becomes larger the time for the first jumping event, from one cell to its neighbor, becomes larger in statistical sense.

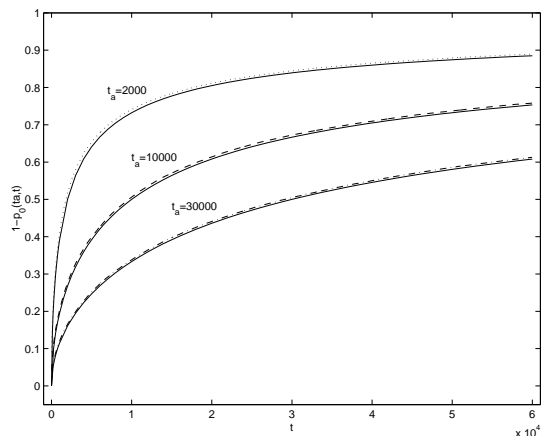


FIG. 2. We show the probability of making at least one step in a time interval $(0, t)$ for different aging times specified in the figure. The solid curve is the theoretical prediction Eq. (10), the dotted, dashed, and dot dashed curves are obtained from numerical solution of the map with $z = 3$.

We now investigate the ACTRW Green function. Let $p_n(t_a, t)$ be the probability of making n steps in the time interval $(0, t)$. Let $P(k, s, u)$ be the double-Laplace – Fourier transform ($x \rightarrow k, t_a \rightarrow s, t \rightarrow u$) of $P(x, t_a, t)$, then

$$P(k, s, u) = \sum_{n=0}^{\infty} p_n(s, u) \cos^n(k), \quad (12)$$

where $p_n(s, u)$ is the double Laplace transform of $p_n(t_a, t)$. In Eq. (12) $\cos^n(k)$ is the characteristic function of a random walk with exactly n steps. Using convolution theorem of Laplace transform

$$p_n(s, u) = \begin{cases} \frac{1 - sh_s(u)}{su} & n = 0 \\ h_s(u)\psi^{n-1}(u)\frac{1-\psi(u)}{u} & n \geq 1. \end{cases} \quad (13)$$

Hence inserting Eq. (13) in Eq. (12), using Eq. (9) and summing we find

$$P(k, s, u) = \frac{1}{su} + \frac{[\psi(u) - \psi(s)][1 - \cos(k)]}{u(u-s)[1 - \psi(s)][1 - \psi(u)\cos(k)]}. \quad (14)$$

We note that only if the underlying process is a Poisson process, the Green function $P(x, t_a, t)$ is independent of t_a .

By differentiating Eq. (14) with respect to k twice and setting $k = 0$, we obtain the mean square displacement of the random walk

$$\langle x^2(s, u) \rangle = \frac{h_s(u)}{u[1 - \psi(u)]} \quad (15)$$

From Eq. (7) we have $\psi(u) = 1 - Au^\alpha \dots$, when u is small. Using Tauberian theorem one can show that for $t, t_a \gg A^{1/\alpha}$

$$\langle x^2(t_a, t) \rangle \sim \frac{1}{A} \frac{1}{\Gamma(1 + \alpha)} [(t + t_a)^\alpha - t_a^\alpha]. \quad (16)$$

For times $t \gg t_a$ we recover standard CTRW behavior, $\langle x^2(t_a, t) \rangle \propto t^\alpha$ [17]. For $t/t_a \ll 1$ we find $\langle x^2(t, t_a) \rangle \propto t/t_a^{1-\alpha}$, hence as t_a becomes larger the diffusion in this regime is slowed down.

This ACTRW behavior is shown in Fig. 3 for the iterated map. We show $\langle x^2(t_a, t) \rangle$ versus time for different values of t_a . Good agreement between ACTRW and the numerical simulations is found. All the curves in Fig. 3 converge into $\langle x^2(t_a, t) \rangle \simeq t^\alpha$ for long forward times t , while at shorter times the diffusion is clearly slowed down as the aging time is increased.

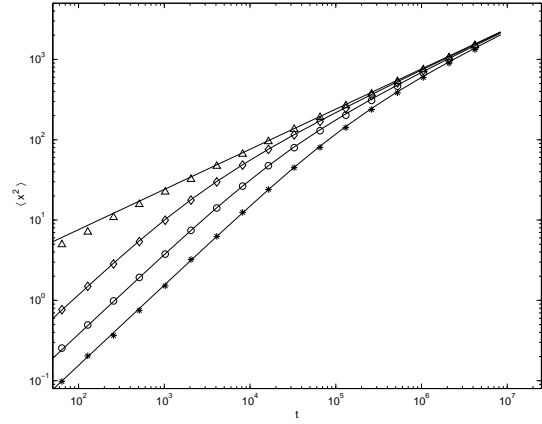


FIG. 3. We show the mean square displacement versus the forward time t for different aging times t_a , $t_a = 0$ triangle, $t_a = 1000$ diamond, $t_a = 10000$ circle, and $t_a = 60000$ star. The solid curves are the theoretical prediction Eq. (16). Here $z = 3$.

To investigate properties of the Green function $P(x, t_a, t)$ in the limit of long t and t_a we consider the continuum approximation of Eq. (14) (soon to be briefly justified). We insert the large wave length expansion $\cos(k) = 1 - k^2/2$ and low frequency expansion $\psi(u) = 1 - Au^\alpha$ in Eq. (14)

$$P(k, s, u) \simeq \frac{s^\alpha u - su^\alpha}{s^{\alpha+1}u(u-s)} + \frac{(u^\alpha - s^\alpha)}{s^\alpha(u-s)} \frac{Au^{\alpha-1}}{Au^\alpha + k^2/2}. \quad (17)$$

Inverting to the double time (t, t_a) – real space x domain we find that the Green function is a sum of two terms:

$$P(x, t_a, t) \sim p_0(t_a, t) \delta(x) + \frac{\sin(\pi\alpha)}{\pi} \frac{1}{t_a \left(\frac{t}{t_a}\right)^\alpha \left(1 + \frac{t}{t_a}\right)} \otimes \frac{t|x|^{-(1+2/\alpha)}}{\alpha(2A)^{1/\alpha}} l_{\alpha/2} \left(\frac{t|x|^{-(2/\alpha)}}{(2A)^{1/\alpha}} \right) \quad (18)$$

where in this limit

$$p_0(t_a, t) \sim \frac{\sin(\pi\alpha)}{\pi} \int_{t/t_a}^{\infty} \frac{dx}{x^\alpha(1+x)}. \quad (19)$$

The first term on the right hand side of Eq. (18) is a singular term. It corresponds to a random walk which did not make a jump in the time interval $(0, t)$. The symbol \otimes in the second term in Eq. (18) is the Laplace convolution operator with respect to the forward time t , $l_{\alpha/2}(t)$ is the one sided Lévy stable PDF, whose Laplace pair is $\exp(-u^{\alpha/2})$. It is easy to see that the asymptotic solution Eq. (18) is non negative and normalized [proof: set $k = 0$ in Eq. (17)]. In the limit $\alpha \rightarrow 1$ we get a Gaussian Green function which is independent of t_a ,

hence in the normal transport regime no aging behavior is found [proof: set $\alpha = 1$ in Eq. (17)].

To justify the approximation Eq. (18) we have calculated the even moments of the ACTRW exactly, in u, s space, using Eq. (14) [i.e., $\langle x^2(s, u) \rangle$ Eq. (15), $\langle x^4(s, u) \rangle$, etc]. Then using Tauberian theorems we can show that for long t and long t_a , the ratio t/t_a being arbitrary, these moments and the moments obtained directly from the approximation Eq. (18) are identical. In this way we have justified the continuum approximation. The details of this calculation and generalizations to other classes of random walks will be published elsewhere.

The behavior of the Green function Eq. (18) is shown in Fig. (4). Not shown is the behavior on the origin which exhibits a singular behavior [i.e, the $\delta(x)$ term in Eq. (18)]. The behavior of this singular term was displayed already in Fig. 2. A good agreement between simulations and the ACTRW Green function is obtained.

Using Eq. (18) we find the non-singular part of the ACTRW on the origin

$$P(x, t_a, t)|_{x=0} = t^{-\alpha/2} g\left(\frac{t}{t_a}\right), \quad (20)$$

where

$$g(x) = x^{\alpha/2} \frac{\sin(\pi\alpha)}{2\pi\Gamma(1-\alpha/2)} \int_0^x dy \frac{(x-y)^{-\alpha/2}}{(1+y)y^\alpha}. \quad (21)$$

Hence we find the asymptotic behaviors

$$P(x, t_a, t)|_{x=0} \sim \begin{cases} \frac{t^{-\alpha/2}}{2\Gamma(\alpha)\Gamma(2-3\alpha/2)} \left(\frac{t}{t_a}\right)^{1-\alpha} & t \ll t_a \\ \frac{t^{-\alpha/2}}{2\Gamma(1-\alpha/2)} & t \gg t_a. \end{cases} \quad (22)$$

In the limit of $t \gg t_a$ we recover the standard CTRW behavior [17]. Note however that the convergence of ACTRW to standard CTRW behavior may become extremely slow when α is small. For example when $\alpha = 1/12$, and $t/t_a = 10^8$, large deviations from the asymptotic limit are found: $2\Gamma(1-\alpha/2)t^{\alpha/2}P(x, t_a, t)|_{x=0} = 0.788$ instead of the asymptotic value 1. Since the limit $\alpha \rightarrow 0$ is important for several systems [18], (i.e., logarithmic diffusion as found in Sinai's model), it is clear that aging can be important also when $t > t_a$.

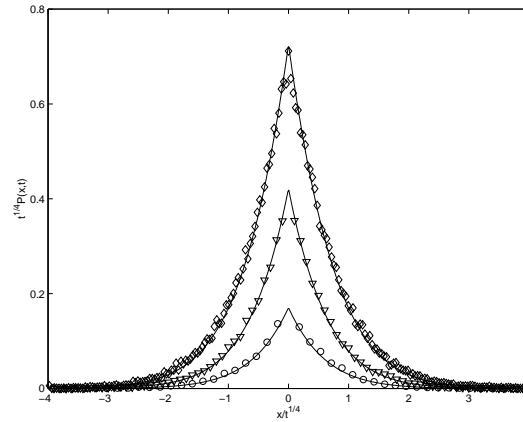


FIG. 4. We show the Green function obtained from simulation of the deterministic map in *scaling form* for: (i) $t_a = 10^4, t = 10^3$, circles, (ii) $t_a = 10^4, t_a = 10^4$, triangles, (iii) and $t = 4 * 10^5, t_a = 0$, diamonds. The curves are our theoretical results which are in good agreement with the simulations with $z = 3$.

To conclude, we have demonstrated for the first time aging behavior in diffusion generated by iterated maps. In the regime $t \leq t_a$ we observe a slowing down of the dynamics as the aging time is increased. In the limit $t \gg t_a$ we obtain previous results, the convergence towards this regime can become extremely slow when α is small. The aging dynamics of the iterated maps exhibits a universal behavior in the sense that the Green function, $P(x, t_a, t)$ does not depend on precise shape of $\psi(t)$ besides the exponent $\alpha = (z-1)^{-1} < 1$. We believe that aging dynamics can be found also in other low dimensional deterministic systems, an issue left for future research.

Acknowledgments I thank J. P. Bouchaud for pointing out Ref. [16] and Yuan-Chung Cheng for helping with the numerics.

-
- [1] L.C.E. Struick, *Physical Aging in Amorphous Polymers and Other Materials* (Elsevier, Houston, 1978).
 - [2] C. Monthus and J. P. Bouchaud, *J. Phys. A* **29**, 3847 (1996).
 - [3] B. Rinn, P. Maass, and J. P. Bouchaud *Phys. Rev. Lett.* **84**, 5403 (2000).
 - [4] J. Klafter, M. F. Shlesinger and G. Zumofen, *Phys. Today* **49** (2) 33 (1996).
 - [5] T. H. Solomon, E. R. Weeks, and H. L. Swinney, *Phys. Rev. Lett.* **71**, 23 (1995).
 - [6] R. Klages, and J. R. Dorfman, *Phys. Rev. Lett.* **74**, 387 (1995).
 - [7] H. G. Schuster, *Deterministic Chaos* (VCH Verlagsgesellschaft mbH, Weinheim 1989). E. Ott, *Chaos in Dy-*

namical Systems (Cambridge University Press, Cambridge, 1993).

- [8] T. Geisel, and S. Thomaе, *Phys. Rev. Lett.* **52**, 1936 (1984).
- [9] T. Geisel, J. Nierwetberg, and A. Zacharel, *Phys. Rev. Lett.* **54**, 616 (1985).
- [10] G. M. Zaslavsky, M. Edelman, and B. A. Niyazov, *Chaos* **7**, 159 (1997).
- [11] M. Schell, S. Fraser, and R. Kapral, *Phys. Rev. A*, bf 26, 504 (1982).
- [12] R. Bettin, R. Mannella, B. J. West, and P. Grigolini, *Phys. Rev. E*. **51**, 212 (1995).
- [13] G. Radons, *Phys. Rev. Lett.* **77**, 23 (1996).
- [14] E. Barkai, and J. Klafter, *Phys. Rev. Lett.* **79**, 2245 (1997).
- [15] G. Zumofen, and J. Klafter, *Phys. Rev. E*. **47**, 851 (19993).
- [16] C. Gordeche, and J. M. Luck, *J. of Statistical Physics* **104** 489 (2001).
- [17] R. Metzler, and J. Klafter, *Phys. Rep.* **339** 1 (2000).
- [18] J. Drager, and J. Klafter, *Phys. Rev. Lett.* **84** 5998 (2000).